analytical chemistry

Technical Note

Spatial Localization and Quantitation of Androgens in Mouse Testis by Mass Spectrometry Imaging

Diego F Cobice, Dawn E. W. Livingstone, Colin Logan Mackay, Richard J. A. Goodwin, Lee B. Smith, Brian R. Walker, and Ruth Andrew

Anal. Chem., **Just Accepted Manuscript** • DOI: 10.1021/acs.analchem.6b02242 • Publication Date (Web): 27 Sep 2016

Spatial Localization and Quantitation of Androgens in Mouse Testis by Mass Spectrometry Imaging

Diego F Cobice[a,§], Dawn EW Livingstone[a,b,§], C Logan Mackay[c], Richard JA Goodwin[d], Lee B Smith[e], Brian R Walker[a] and Ruth Andrew[a]*

[a] University/British Heart Foundation Centre for Cardiovascular Science, Queen´s Medical Research Institute, University of Edinburgh, 47 Little France Crescent, Edinburgh, EH16 4TJ, UK, [b] Centre for Integrative Physiology, University of Edinburgh, Hugh Robson Building, 15 George Square, Edinburgh EH8 9XD, UK. [c] SIRCAMS, School of Chemistry, University of Edinburgh, Joseph Black Building, The King's Buildings, West Mains Road, Edinburgh, EH9 3JJ, UK.[d] AstraZeneca R&D, Cambridge, CB4 0WG, UK.[e] MRC Centre for Reproductive Health; Queen´s Medical Research Institute, University of Edinburgh, 47 Little France Crescent, Edinburgh, EH16 4TJ, UK. $ Joint first author

Corresponding Author: Professor Ruth Andrew. as above

Tel: +44 (0) 131 242 6763

Fax: +44(0) 131 242 6779

Email: ruth.andrew@ed.ac.uk

* Footnote: Subsequently Biomedical Sciences Research Institute, School of Biomedical Sciences, University of Ulster, Coleraine campus, Cromore Road, Coleraine, Co. Londonderry, BT52 1SA, UK.

Abstract

Androgens are essential for male development and reproductive function. They are transported to their site of action as blood-borne endocrine hormones, but can also be produced within tissues to act in intracrine and paracrine fashions. Because of this, circulating concentrations may not accurately reflect the androgenic influence within specific tissue microenvironments. Mass spectrometry imaging permits regional analysis of small molecular species directly from tissue surfaces. However, due to poor ionization and localized ion suppression, steroid hormones are difficult to detect. Here derivatization with Girard T reagent was used to charge-tag testosterone and 5α-dihydrotestosterone allowing direct detection of these steroids in mouse testes, in both basal and maximally-stimulated states and in rat prostate. Limits of detection were ~0.1 pg for testosterone. Exemplary detection of endogenous steroids was achieved by matrix-assisted laser desorption ionization and either Fourier transform ion cyclotron resonance detection (at 150 μm spatial resolution) or quadrupole-time of flight detection (at 50 μm spatial resolution). Structural confirmation was achieved by collision induced fragmentation following liquid extraction surface desorption and electrospray ionization. This application broadens the scope for derivatization strategies on tissue surfaces to elucidate local endocrine signaling in health and disease.

Introduction

Androgens are essential regulators of male development and adult reproductive function, primarily synthesized within the testis. During embryonic development, testicular fetal Leydig and Sertoli cells work in concert to produce testosterone[1;2]. This is converted into the most active androgen, 5α-dihydrotestosterone (DHT), by 5α-reductases in peripheral tissues to promote masculinization and normal size of target organs[3-5]. In postnatal life a second population of (adult) Leydig cells develops superseding the fetal population; these Leydig cells complete all steps of steroidogenesis to produce and secrete testosterone throughout adulthood[6]. Additional androgens, androstenedione (A4) and dehydroepiandrosterone (DHEA), are synthesized in the adrenal glands in many species but not rats or mice[7;8]. Androgens have pleiotropic functions in the testis, e.g. completion of meiosis, differentiation of spermatids, initiation of spermatogenesis at puberty and maintenance of this process in the adult[9]. Dysregulation of these processes may lead to testicular dysfunction and infertility. In contrast, increased androgen signaling plays a role in pathologies, including benign prostatic hyperplasia (BPH) and prostate cancer [10;11]

Liquid chromatography-tandem mass spectrometry (LC-MS/MS) is the method of choice for quantifying circulating androgens, but little information is available relating circulating to tissue levels due to analytical limitations. While androgens may be quantified in extracts of biopsies[7;12], this does not spatially align steroid levels with sub-regions, e.g. cell types or tumours. Retaining spatial distribution of androgens can be crucial, for examples in androgen-sensitive prostate tumours, where the cellular activities of 5α-reductases are critical to the local exposure to DHT. Mass spectrometry imaging (MSI) is gaining traction as a bioanalytical tool to map spatial distribution of small molecules in tissues and identify, localize and relatively quantitate compounds in complex biological matrices[13]. Many small

molecule applications of MSI pertain to drug discovery, but we recently validated a MSI approach for assessing the spatial distribution of glucocorticoids in murine brain[14]. On-tissue chemical derivatization (OTCD) using Girard T (GirT) reagent overcame poor target ionization efficiency, ion suppression and the increased *m/z* helped avoid interference of matrix-related background in the lower mass range. GirT reagent reacts with ketones[15] and enhances sensitivity in the measurement of lipophilic steroids within tissue matrix, but the approach requires skillful and flexible manual application. Glucocorticoids are pregnene steroids, with several ketones, the most reactive being at C3 in the A-ring, conjugated with a C4-5 double bond (Supporting Information: Nomenclature of steroids, Figure S-1). The endogenous androgens, testosterone and androstenedione, contain a similar ketonic function and may also be derivatized using hydrazine-based reagents[15] (Supporting Information: Derivatization Reactions, Figure S-1). A recent report suggests derivatization with GirT is useful for MSI of testosterone in tissue[16]. However, within tissue, testosterone levels must be interpreted in conjunction with those of the more potent DHT. The A-ring of DHT is reduced and the ketone less activated (not allylic to the Δ4-5 double bond) and thus less amenable to derivatization.

Here we describe how OTCD with MSI can spatially localize testosterone and DHT in rodent reproductive tissues. Translational challenges and methodological improvements to reduce diffusion and increase robustness by inclusion of automated spraying technology are reported for the first time.

Experimental

***Sources of Chemicals*:** Internal standard [^{2}H]$_8$-corticosterone-2,2,4,6,6,7,21,21 (d_8-CORT, Cambridge Isotopes; MA, USA); unlabeled steroids (Steraloids Inc, PA, USA). Solvents were glass-distilled HPLC grade (Fisher Scientific, Loughborough, UK). Other chemicals were from Sigma-Aldrich (Dorset, UK) unless stated. Room temperature (RT) was 18-21°C.

Animals and biomatrix collection: C57BL/6 mice (Harlan Olac Ltd, Bicester, UK) were studied under UK Home Office license. To stimulate androgen biosynthesis, human chorionic gonadotrophin (hCG, 20 IU, Organon, The Netherlands) or vehicle (saline) was administered by subcutaneous injection to male mice (aged 8-10 weeks; n=3/group) and testes and blood collected following cull by CO_2 16 h later. Plasma (EDTA) was prepared by centrifugation (10,000 g, 5 min, 4°C). Tissues were snap frozen in liquid nitrogen and stored (-80˚C). Concentrations of testosterone in plasma were quantified by LC-MS/MS[17]. Prostates were similarly collected from male Sprague Dawley rats (Harlan Olac Ltd).

Reaction efficiency: LC-MS/MS analysis of non-derivatized and derivatized steroids: Steroid (1 µg/10 µL methanol) was derivatized with GirT (5 mg/mL in methanol containing 0.1% trifluroacetic acid (TFA)) by heating (40°C, 60 min) and the reaction stopped with water (50 µL). Non-derivatized and derivatized steroids were analyzed by LC-MS/MS (QTrap 5500 triple quadrupole MS (Sciex, Warrington, UK) interfaced with an Acquity UPLC (Waters, Manchester, UK)). Separation was achieved using a Kinetix C18 column (Phenomenex, Macclesfield, UK; 150 cm, 3 mm, 2.6 µm; 35°C). Initial mobile phase conditions were water with 0.1% formic acid:methanol (70:30), changing to 20:80 from 1-10 minutes and then sustained until 15.5 minutes. Selected ion monitoring detected non-derivatized and derivatized steroids respectively; testosterone (*m/z* 289.1, 402.3) and DHT (*m/z* 291.1, 404.2) with electrospray (ESI) MS (source temperature 30°C, ion source gases (GS1, GS2 50 and 70

respectively), CAD Low, ion spray voltage 5500 V, curtain gas 40 psi, entrance potential, 10 V).

Imaging Instrumentation: MSI was performed firstly, by 12T SolariX MALDI-FTICR-MS (Bruker Daltonics, MA, US) employing a Smartbeam 1 kHz laser, operated with SolariX control v1.5.0 (build 42.8), Hystar 3.4 (build 8) and FlexImaging v3.0 (build 42). Confirmatory on-tissue collision induced dissociation (CID) was carried out by Liquid extraction surface analysis (LESA)-nanoESI-FTICR-MS (Triversa Nanomate®, Advion, New York, USA). Secondly high spatial resolution imaging was performed using a MALDI q-TOF MS (MALDI Synapt G2 HDMS, Waters). Regions of interest (ROIs) were defined. Image files were generated in Mass Lynx (v4.1), then viewed in HDI Imaging (v1.2).

***Tissue sectioning and mounting*:** Tissue was embedded in gelatin (50 %*w/v)*. Top-down (horizontal) sections of testes (10 µm) were thaw mounted onto conductive indium tin-oxide (ITO)-coated glass slides (Bruker Daltonics, Bremen, GmbH) and stored in a vacuum desiccator (RT, 1 h) and then at -80˚C. Adjacent sections were stained using haematoxylin and eosin. After fixation in cold acetone, tissue sections were examined using an optical microscope (40X, Leica Microsystems Inc, Bannockburn, IL, USA) with CCD camera (Hitachi, 3969, Japan).

Detection of endogenous steroids in rodent tissues without derivatization: Tissues were prepared and matrix applied (α-cyano-4-hydroxycinnamic acid; CHCA) as below.

Detection of endogenous steroids in rodent tissues following OTCD: From -80°C, tissue sections were dried in a vacuum desiccator (20 mins). Derivatization reagent (GirT, 5 mg/mL methanol: water (80:20) with 0.1% TFA containing d_8-CORT (10 µg/mL) was applied by artistic airbrush[14], with a reagent density of 0.11 mg/cm^2. The procedure for reagent and matrix application[14] was automated for higher resolution imaging. The reagent was applied

(flow rate 90 µL/min) by automated sprayer (HTX Technologies, Carrboro, North Carolina, US). Nebulization gas was nitrogen (10 psi). The nozzle spray (100°C, positioned ~35 mm from the target) was deposited (linear velocity 850 mm/min, offset spacing 3 mm). Ten passes were performed leading to a matrix density of 0.21 mg/cm^2, matched to manual spraying[14]. On alternate passes, the spray pattern was offset by 1.8 mm. After derivatization, the slide was placed in a temperature/humidity controlled chamber (Memmert HPP 110, Schwabach, GmbH; 40°C, 80% relative humidity) in a sealed slide box. The tissue was incubated (60 min, 40°C), then allowed to cool and dry in a vacuum desiccator (RT, 15 min) to remove the condensed water prior to matrix deposition.

Matrix application: CHCA (10 mg/mL in acetonitrile (80%) + 0.2% v/v TFA) was applied by a pneumatic TLC sprayer (20 mL/slide, nitrogen flow 7.5 L/min, distance 20 cm from target). Each manual pass took ~1 s and was repeated with 5-10 s between passes, until uniform coating was achieved. The tissue section was allowed to dry (RT) and stored in a desiccator. For higher resolution studies, the matrix was applied by automated sprayer as above except that the nozzle was 90°C and linear velocity 1100 mm/min.

MALDI-FTICR-MSI analysis: Optical images were scanned (Canon LiDE-20, Canon, UK). MSI analysis was performed using constant accumulation of selected ions (CASI™) using a 80 Da isolation window centered at 435 Da yielding a 2 Mword time-domain transient. Laser spot diameter was 100 µm and raster spacing 100–300 µm. Laser shots were 800 and power optimized for consistent ion production. MSI data were subject to window normalization to *m/z* of 468.3064 (GirT-d_8-CORT). Mass precision was typically ±0.0005 Da. Average abundances was assigned from the summed spectra within ROIs. Neutral testosterone and DHT were analyzed (without derivatization) in positive mode at *m/z* 289.2098 and *m/z* 291.2112. Ions of derivatives were monitored in positive mode; *m/z* 402.3115 (GirT-

testosterone) and 404.3271 (GirT-DHT). The CHCA matrix ion at +ve *m/z* 417.0483, along with GirT-d_8-CORT, were monitored to assess uniformity of matrix application.

Higher Spatial Resolution Analysis: Using a MALDI q-TOF MS, the ROI was defined and the spatial resolution set (50 µm). Positive ion data were acquired in sensitivity mode (target enhancement at *m/z* 402) with 350 laser shots/raster position using a 1 kHz laser. Optimization was achieved by tuning acquisition settings while collecting data from a control spot of analytes (0.5 µL, 0.1 g/mL of standard at ~2 µm manually spotted with equal volume of derivatization solution/matrix). Ions formed by derivatives were monitored in positive mode; *m/z* 402.31 (GirT-testosterone), *m/z* 404.33 (GirT-DHT). Mass filter windows were selected with a precision of ±0.04 Da. Data were normalized by total ion current.

Liquid extraction surface analysis (LESA)-ESI-FTICR-MS: Steroids within tissue sections were derivatized[14] and analyzed immediately using LESA-nanoESI-FTICR-MS with the 12T SolariX ESI-MALDI source; solvent (methanol: water, 50:50 with 0.1% v/v of formic acid), pick-up volume: 1.5 µL, dispense volume, 1.2 µL at 0.2 mm from surface, droplet rest time (delay) 5 s and aspiration volume of 1.4 µL at 0.0 mm from surface. Ions were detected between *m*/*z* 250-1500, with an isolation window of 0.1 Da, yielding a 2 Mword time-domain transient. Ions of GirT-hydrazones (as MALDI) were isolated (30 s) prior to selection of *m*/*z* 400.3±5 for CID performed at 32 eV.

Limits of Detection were assessed by spotting serial dilutions of steroid solutions (0.1–100 pg) onto slides and also control sections (murine brain) and assessed by MALDI-FTICR-MS.

Data were compared using Student's *t*-test (Statistica® version 8.0, StatSoft, Inc., Tulsa, OK, USA).

Results and Discussion

***Mass Spectral Characterization of Steroids*:** The mass spectra of non-derivatized androgen standards contained protonated molecular ions (testosterone *m/z* 289.2098*;* DHT *m/z* 291.2112). Initial imaging attempts to detect non-derivatized androgens in mouse testes were unsuccessful, as signal to noise ratios (SNR) <2 (**Figures 1b, 1g**), even following hCG stimulation. This resembles glucocorticoids, which are also undetectable in their native state by ourselves[14] and others[16]. Accordingly, GirT derivatives were formed and reactions monitored using ESI, which allowed concomitant assessment of native and derivatized forms. With ESI, the steroid signal intensities were boosted by ~20-30x by derivatization. However, reaction efficiencies differed with DHT, reacting ~5 times more slowly than testosterone, due to its less reactive 3-ketone.

Reaction conditions were subsequently optimized on-tissue using testosterone. The MALDI MS spectra of the GirT-hydrazones yielded $[M]^+$ ions, with masses at *m*/*z* 402.3114 for testosterone (**Figure 1k**) and *m*/*z* 404.3264 for DHT (**Figure 1l**), in close agreement with theoretical masses. As before, GirT derivatives yielded spectra dominated by the molecular ion and high resolution MS overcame the challenge of selecting specific analytes from high abundance ions in the low mass range emanating from matrix and tissue. Structural confirmation was performed within tissue by CID using LESA-ESI-FTICR-MS, allowing isolation experiments to be performed with greater sensitivity than could be achieved during MALDI imaging (Supporting Information: CID mass spectra, Figure S-2). CID of GirT-testosterone generated fragment ions (*m/z* 343 and 315) characteristic of loss of the quaternary amine tag $[M-59]^+$ and carbon monoxide $[M-87]^+$ respectively from the derivatized group. Similar fragmentation occurred with GirT-DHT. Proposed patterns (Supporting Information: Proposed Fragmentation Patterns, Figures S-2) agreed with the fragmentations of GirT

derivatives of glucocorticoids[14] and also those of GirP steroid hydrazones, which may form stable five membered rings[18]. Further androgens (androstenedione, DHEA) were also successfully derivatized with GirT (Supporting Information: Mass spectrum, Figure S-3). Notably GirT-DHEA gave the same precursor ion as testosterone and fragmented similarly under LESA conditions, unless high energy was applied.

OTCD and matrix application were adapted for automated spraying, allowing greater control of crystal size and topological homogeneity, aiming to improve spatial resolution and reduce the likelihood of hot spots. Previously deposition of methanolic solutions was by either manual TLC sprayer or air-brushes, where distance from target and nozzle-nozzle reproducibility were difficult to control, varying between suppliers and even lots. Nonetheless a good spray mist could be achieved leading to a homogenous layer of reagent, good analyte extraction and desirable co-crystallization. However, reproducibility was highly analyst dependent and analyte diffusion was a concern through repeated wetting.

Sublimation (solvent-free) was piloted, leading to smaller crystals size but poor tissue-extraction, particularly with hydrophobic analytes. Shimma et al report a successful dual approach of sublimation and airbrush to reduce crystal size[16]. Ultimately automated deposition was used, improving reproducibility and crystal size homogeneity but requiring extensive optimization of spray parameters (nozzle temperature, nitrogen flow, solvent composition, solvent flow rate, surface tension) to achieve good analyte extraction. A balance between “not too wet”, promoting diffusion, and “not too dry”, impeding analyte extraction, was struck. Our experience is that, while reproducibility is improved by automated spraying, better sensitivity/extraction may still be observed using air-brush. Furthermore, automatic sprayers require instrument-specific optimization.

Relative quantitation of derivatized steroids: CASI was used to maximize signal intensity and limits of detection (LODs) of derivatized testosterone were ~ 0.1pg (off-tissue) and 1pg (on-tissue; SNR 21). GirT derivatives of testosterone yielded ions of similar intensity to GirT-d8-CORT; similar ionization efficiency is anticipated[14], for steroids with an activated A-ring ketone. However, the yield of GirT-DHT was lower due to reduced reactivity of the non-conjugated ketone moiety. Therefore relative quantitation between testosterone and DHT requires normalization, readily achievable with stable-isotope labeled internal standards. ^{13}C labelling is preferred to deuterium due to the potential for loss of deuterium during derivatization or fragmentation[19].

Detection of endogenous steroids in rodent tissues

GirT derivatives of androgens were successfully detected using two imaging MS platforms. Initially studies were performed by MSI (with FTICR) at 150 µm spatial resolution in murine testes, detecting steroids with mass accuracy of ±5 ppm from their theoretical mono-isotopic mass **(Figure 1k, 1l).** Androgens were detected in control testes (**Figures 1c, 1h**) with SNR of 22±5 and 43.5±4 for derivatized testosterone and DHT respectively. Testosterone and DHT were in higher abundance following stimulation with hCG (**Figures 1d, 1i**); SNR 265±11 and 387±13 respectively. The absolute signal intensity of testosterone and DHT relative to d_8CORT were increased ~2.5 and ~1.8 fold by hCG (**Figure 2e, 2j**) respectively. Corresponding concentrations of testosterone in plasma rose from 4.5±0.7 to 29.6±1.8 nM following hCG, typical of the protocol[20]. Shimma et al reported an increase of greater magnitude, but over a shorter timecourse[16].

The distributions of testosterone and DHT following hCG stimulation were assessed at higher spatial resolution (50 µm) using a MALDI-q-TOF instrument. In CASI mode on the SolariX (800 laser shots/pixel) a decline in sensitivity after 20000 pixels was observed, possibly due to an accumulation of matrix/reagent ion clusters in the source; this was not observed by

qTOF-MS. The steroid derivatives yielded the same molecular ions as with FTICR. The mass resolution was ~20000 (at *m/z* 400) as opposed to 350000 and the difference in mass accuracy of selected ions was <5 ppm versus their theoretical monoisotopic masses (**Figure 2g**). Potential interfering ions within the mass window were not evident in either the qTOF or the FTICR spectra from mouse testes. DHT was also detected, but with a different spatial distribution. Testosterone was mainly localized within the seminiferous tubules (**Figure 2a, 2d**), whilst DHT was mainly observed in the interstitium/Leydig cells (**Figure 2b, 2e**). Although Shimma et al[16] report Leydig cell localization of testosterone, their images display a clear signal in seminiferous tubules, in keeping with ours.

The method was subsequently applied to prostate tissue. 5α-Reductases are pharmacological targets within prostate, since suppression of DHT production attenuates growth of both hyperplastic and cancerous tissue. Both testosterone and DHT could be detected SNR>10 (**Figures 1n,1o,1p**), suggesting that the MSI approach may open doors to pathological investigations of cell-specific androgen synthesis in prostate disease.

Conclusions

Derivatization permits detection of poorly ionizable endogenous androgens in target tissues by MSI. The use of Gir T reagent affords low limits of detection, similar to glucocorticoids[14]. OTCD proceeded rapidly for testosterone but was less efficient for DHT. However both were detected in tissue. For relative quantitation, commercial stable-isotope labeled androgens would allow data collection within a narrower mass window of ± 5 or 10 Da, (as opposed to 80 Da using d_8CORT), potentially improving sensitivity.

OTCD coupled with MALDI-FTICR-MSI successfully detected androgens in murine testes. A proof-of-principle experiment, representative of healthy biological variations in tissue steroid levels, was performed using hCG to maximally stimulate androgen synthesis, achieving an increase in plasma testosterone which was also reflected in testicular steroids. Initial studies were performed at 150 μm resolution, detecting androgens in testes but without meaningful molecular histology. The seminiferous tubules of mice are ~300 μm in diameter and hence smaller laser bores were required to reveal the characteristic tissue structure, although this may be less challenging in larger species. Higher resolution imaging (50μm), localized testosterone and DHT to different compartments of the adult mouse testis.

The need for higher resolution imaging brings with it concerns over analyte diffusion, matrix crystal size and tissue integrity. Manual application of matrix and reagent, while effective, was subject to variability between operators. The automated application allows better tissue-tissue reproducibility and improved homogeneity of matrix coverage compared with TLC sprayers or airbrushes. Future optimization of OTCD and matrix application by sublimation may allow even higher spatial resolution, possibly 5 μm approaching cellular resolution, now obtainable with new MALDI systems.

MSI with OTCD is a powerful tool to study the regional variation in abundance of androgens in tissues and here we broaden scope of the technique to reproductive biology. In translating to non-rodent tissues, the presence of isobaric steroids, highly abundant DHEA, as well as epi-testosterone, must be considered. Although underivatized DHEA fragments differently from testosterone under tandem MS conditions, the predominant fragment of the derivatives within FTICR or the qTOF is the derivatizing group, militating against their discrimination in the absence of chromatography. Other approaches such as MSn as reported with the IMScope®[16] or ion mobility may permit isomeric separation, as required by translational research.

Acknowledgements

We acknowledge funding from the Medical Research Council (MC_PC_12014), the British Heart Foundation (RG-05-008) and its Centre for Research Excellence (BHF RE/08/001). BRW is a Wellcome Trust Senior Investigator.

Conflict of Interest Disclosure

No conflicts of interest to declare.

Figure captions

Figure 1

Molecular imaging by MALDI-FTICR-MSI of androgens analyzed intact and as Girard T derivatives in murine testes. Non-derivatized steroids could not be detected testes even following stimulation with human chorionic gonadotrophin (hCG). However, upon derivatization, testosterone and 5α-dihydrotestosterone (DHT) were detected. Optical images of a cryosection of murine testis (**a, f**) or rat prostate **(m).** Molecular image of: (**b**) non-derivatized testosterone at *m/z* 289.2098±0.005Da in an hCG-stimulated mouse. Derivatized testosterone at *m/z* 402.3114±0.0005Da in testes from (**c**) control and (**d**) hCG stimulated mouse. (**e**) The relative abundance of testosterone (corrected for internal standard, d8-corticosterone (d8-CORT)) was increased ~2.5 fold following hCG stimulation. Molecular image of: (**g**) non-derivatized DHT at *m/z* 291.2112±0.0005Da in an hCG stimulated mouse. Derivatized DHT at *m/z* 404.3264±0.0005Da in testes from (**h**) control and (**i**) hCG stimulated mouse. (**j**) The relative abundance of DHT (corrected for internal standard) was increased ~1.8 fold following hCG stimulation. Derivatised testeosterone **(n)** and DHT **(o)** in rat prostate. Representative FTICR-MS spectrum of **(k)** testosterone and **(l)** DHT hydrazone in mouse testes and **(o)** both steroidal derivatives in rat prostate showing excellent agreement (mass accuracy ±5 ppm) with simulated theoretical isotopic distribution pattern (embedded). Data are mean±SEM; n=3 mice per group. **cps** = counts per second. Scale bar (2 mm). Signal intensity is depicted by color on the scale shown. ** = $p<0.01$ compared by Student *t*-test.

Figure 2

Molecular imaging of testosterone and 5α-dihydrotestostrone (DHT) Girard T derivatives in rodent testes at 50 µm spatial resolution by MALDI-qTOF-MSI. Images of testes from mice stimulated with human chorionic gonadotrophin (**a**) Derivatized testosterone

at *m/z* 402.31±0.02Da. (**c**) 15X zoom image of (a) (**b**) Derivatized DHT at *m/z* 404.33±0.02Da (**d**) 15X zoom image of (b). (**e**) 15X zoom of haematoxylin and eosin stained section of mouse testis. (**f**) cartoon of testicular architecture (ST = seminiferous tubule, LC = Leydig cells. **(g) (j)**. Mass Spectra of steroid derivatives detected in testes detected by MALDI-qTOF-MSI. Signal intensity is depicted by color on the scale shown. Scale bar (2mm).

Supporting Information

Figure S-1: Steroid Nomenclature and Derivatization Reaction Schemes to form Girard T derivatives of common endogenous androgens.

Figure S-2: Mass spectra and proposed fragmentation patterns of Girard T-derivative of testosterone and dihydrotestosterone collected following liquid extraction surface analysis with nanoESI-FTICR collision induced dissociation.

Figure S-3: MALDI-FTICR-MS spectra and collision-induced fragmentation of a mixture of androstenedione and dehydroepiandrosterone derivatized with Girard T reagent.

Reference List

1. O'Shaughnessy, P.J.; Baker, P. J.; Heikkila, M.; Vainio, S.; McMahon, A.P., *Endocrinology*. **2000,** *141,* 2631-2637.
2. Shima, Y.; Miyabayashi, K.; Haraguchi, S.; Arakawa, T.; Otake, H.; Baba, T.; Matsizaki, S.; Shishido, Y.; Akiyama, H.; Tachibana, T.; Tsutsui, K.; Morohashi, K., *Mol. Endocrinol*. **2013**, *27*, 63-73.
3. Mahendroo, M.S.; Cala, K.M.; Hess, D.L.; Russell, D.W., *Endocrinology*, **2001**, *142*, 4652-4662.
4. Imperato-McGinley, J., *European Urology* **1994**, *25*, 20-23.
5. Bartsch, G.; Rittmaster, R.S.; Klocker, H., *World Journal of Urology,* **2016***, 19*, 413-425.
6. Wen, Q.; Cheng, C.Y.; Liu, Y.X., *Seminars in Cell and Developmental Biology* **2016** DOI.10.1016/j.semcdb.2016.03.003.
7. Labrie, F., *Seminars in Reproductive Medicine* **2004**, *22*, 299-309.
8. Longcope, C., *Menopause* **2016**, *10*, 274-276.
9. Smith, L.B.; Walker, W.H., *Seminars in Cell and Developmental Biology* **2014**, *30*, 2-13.
10. Carson, C., III; Rittmaster, R., *Urology* **2003**, *61*, 2-7.
11. Schitz-Drager, B.J.; Fischer, C.; Bismarck, E.; Dorsam, H.J.; Lummen, G., *Urologe A* **2007,** *46*, 1366-1368.
12. Miyoshi, Y.; Uemura, H.; Umemoto, S.; Sakamaki, K.M.S.; Suzuki, K.; Shibata, Y.; Masumori, N.; Ichikawa, T.; Mizokami, A.; Sugimura, Y.; Nonomura, N.; Sakai, H.; Honma, S.; Harada, M.; Kubota, Y., *BMC Cancer* **2014**, *14,* 717.
13. Heeren, R.M.; Chughtai, K., *Chem Rev* **2010,** *110*, 3237-3277.
14. Cobice, D.F.; MacKay, C.L.; Goodwin, R.; McBride, A.; Langridge-Smith, P.; Webster, S.P.; Walker, B.R.; Andrew, R., *Analytical Chemistry* **2013**, *85*, 11576-11584.
15. Shackleton, C.H.; Chuang H.; Kim, J.; de la Torre X; Segura J, *Steroids* **1997**, *62,* 523-529.
16. Shimma, S.; Kumada, H.-O.; Taniguchi, H.; Konno, A.; Furuta, K.; Matsuda, T.; Ito, S., *Analytical Bioanalytical Chemistry* **2016**, DOI 10.1007/S00216-016-9594-9.
17. Upreti, R.; Faqehi, A.M.M.; Hughes, K.A.; Stewart, L.H.; Walker, B.R.; Homer, N.Z.M.; Andrew R, *Talanta* **2015**, *131*, 728-735.
18. Griffiths, W.J.; Wang, Y., *Biochim.Biophys.Act*. **2011**, *1811*, 784-799.
19. Faqehi, A.M.M.; Cobice, D.F.; Naredo, G.; Mak, T.C.S.; Upreti, R.; Gibb, F.W.; Beckett, G.J.; Walker, B.R.; Homer, N.Z.M.; Andrew R., *Talanta* **2016**, *151,* 148-156.
20. Rebourcet, D.; Wu, J.; Cruickshanks, L.; Smith, S.E.; Milne, L.; Fernando, A.; Wallace, R.J.; Graym C.D.; Hadoke, P.W.F.; Mitchell, R.T.; O'Shaughnessy, P.J.; Smith, L.B., *Endocrinology* **2016***, 157*, 2479-2488.

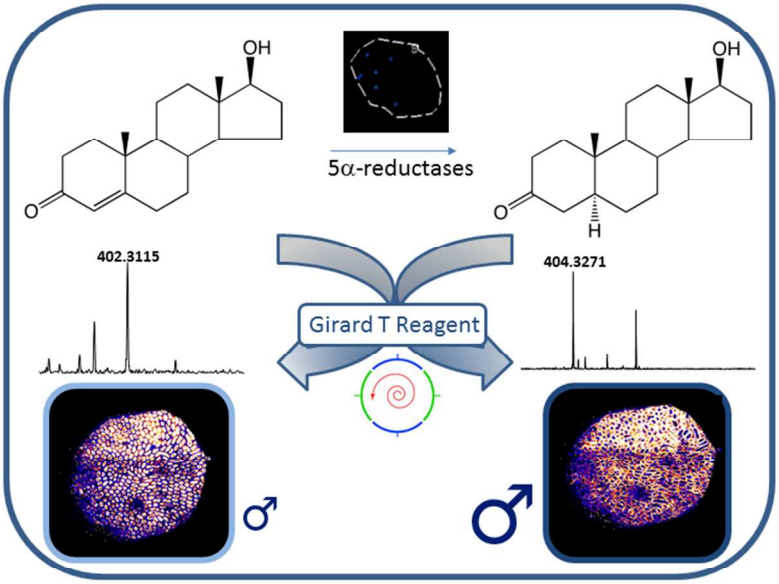

Graphical abstract TOC

254x190mm (96 x 96 DPI)

Figure 1 Cobice et al

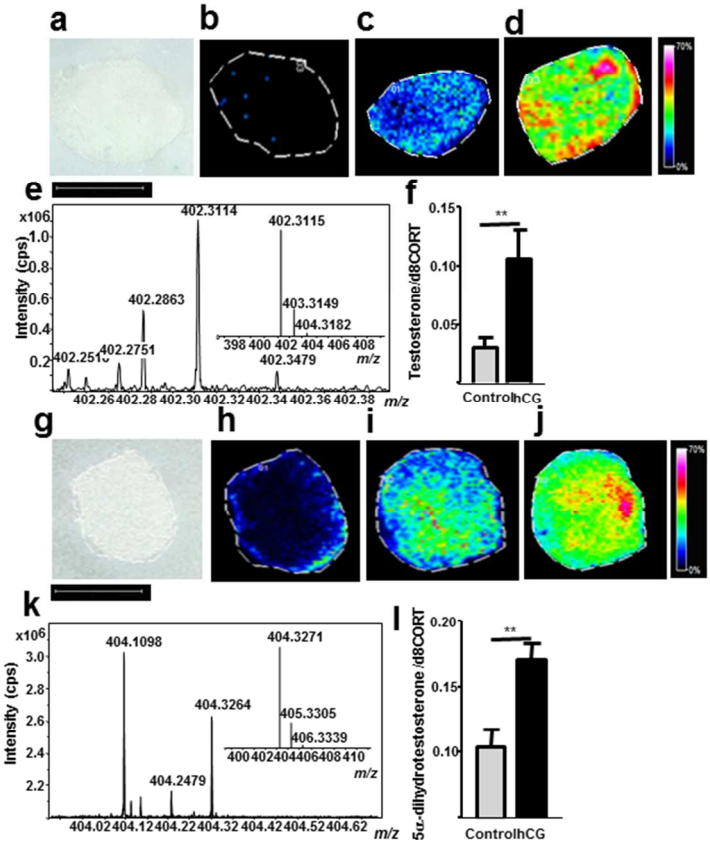

Molecular imaging by MALDI-FTICR-MSI of androgens analyzed intact and as Girard T derivatives in murine testes. Non-derivatized steroids could not be detected testes even following stimulation with human chorionic gonadotrophin (hCG). However, upon derivatization, testosterone and 5α-dihydrotestosterone (DHT) were detected. Optical images of a cryosection of murine testis (a, f) or rat prostate (m). Molecular image of: (b) non-derivatized testosterone at m/z 289.2098±0.005Da in an hCG-stimulated mouse. Derivatized testosterone at m/z 402.3114±0.0005Da in testes from (c) control and (d) hCG stimulated mouse. (e) The relative abundance of testosterone (corrected for internal standard, d8-corticosterone (d8-CORT)) was increased ~2.5 fold following hCG stimulation. Molecular image of: (g) non-derivatized DHT at m/z 291.2112±0.0005Da in an hCG stimulated mouse. Derivatized DHT at m/z 404.3264±0.0005Da in testes from (h) control and (i) hCG stimulated mouse. (j) The relative abundance of DHT (corrected for internal standard) was increased ~1.8 fold following hCG stimulation. Derivatised testeosterone (n) and DHT (o) in rat prostate. Representative FTICR-MS spectrum of (k) testosterone and (l) DHT hydrazone in mouse testes and (o) both steroidal derivatives in rat prostate showing excellent agreement (mass accuracy ±5

ppm) with simulated theoretical isotopic distribution pattern (embedded). Data are mean±SEM; n=3 mice per group. cps = counts per second. Scale bar (2 mm). Signal intensity is depicted by color on the scale shown. ** = $p<0.01$ compared by Student t-test.

190x254mm (96 x 96 DPI)

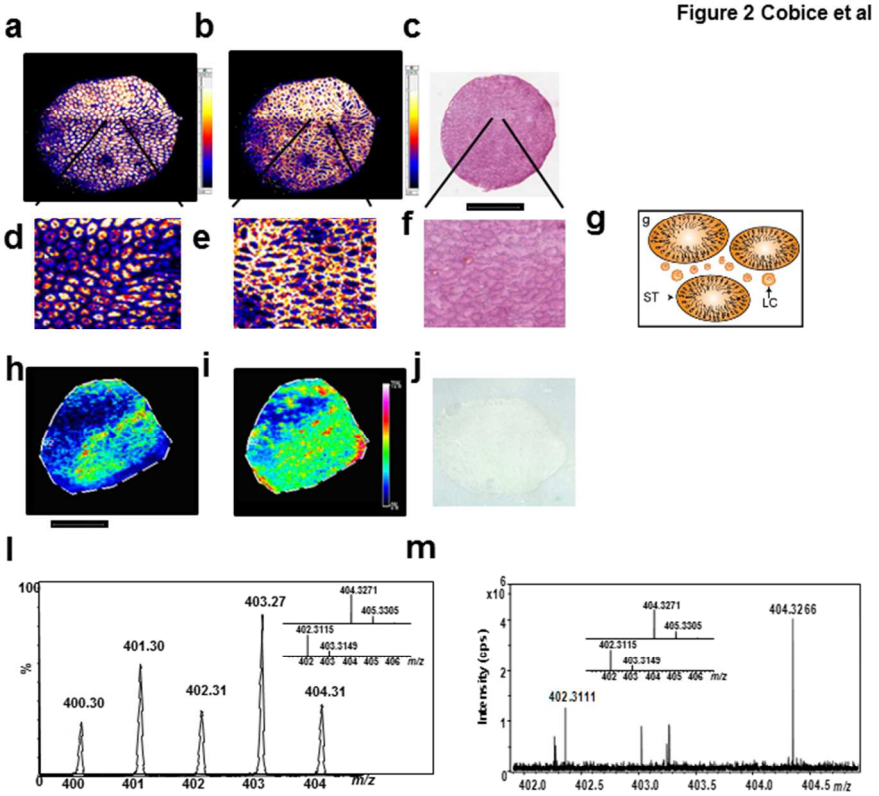

Molecular imaging of testosterone and 5α-dihydrotestostrone (DHT) Girard T derivatives in rodent testes at 50 μm spatial resolution by MALDI-qTOF-MSI. Images of testes from mice stimulated with human chorionic gonadotrophin (a) Derivatized testosterone at m/z 402.31±0.02Da. (c) 15X zoom image of (a) (b) Derivatized DHT at m/z 404.33±0.02Da (d) 15X zoom image of (b). (e) 15X zoom of haematoxylin and eosin stained section of mouse testis. (f) cartoon of testicular architecture (ST = seminiferous tubule, LC = Leydig cells. (g) (j). Mass Spectra of steroid derivatives detected in testes detected by MALDI-qTOF-MSI. Signal intensity is depicted by color on the scale shown. Scale bar (2mm).

190x254mm (96 x 96 DPI)